Thermotropic Liquid Crystalline Poly(organophosphazene)

Robert E. Singler* and Reginald A. Willingham†

Polymer Research Branch, U.S. Army Materials Technology Laboratory, Watertown, Massachusetts 02172-0001

Claudine Noel,*,‡ Claude Friedrich,‡ and Louis Bosio§

Laboratoire de Physicochimie Structurale et Macromoleculaire and Laboratoire de Physique des Liquides et Electrochimie, 10 rue Vauquelin, 75231 Paris Cedex 05, France

Edward Atkins*

H. H. Wills Physics Laboratory, University of Bristol, Tyndall Avenue, Bristol BS8 1TL, U.K.

Received February 5, 1990; Revised Manuscript Received July 2, 1990

ABSTRACT: The liquid crystalline behavior of a poly(organophosphazene) with two 2-(((4-*n*-butylphenyl)-azo)phenoxy)ethoxy side chains per phosphorus atom has been investigated by differential scanning calorimetry, polarized optical microscopy, and X-ray diffraction. On cooling from the isotropic liquid (above 185 °C) a viscous mesophase is first observed which shows the characteristic focal conic texture typical of low molar mass smectic A phases. As the temperature falls below 160–155 °C, a smectic C-like mesophase appears. In these structures, pairs of side chains decorate the backbone at ca. 2.45-Å intervals, and this congestion can be relieved in the cis–trans (2_1 helix) conformation when the stacking periodicity becomes 4.9 Å. In the smectic phases it is likely that the backbone disorders sufficiently to allow the mesogenic side groups to stack and, aided by the flexible spacer, allow the creation of layers perpendicular to the stacking direction. In the smectic A phase, the layer thickness is ca. 25.5 Å, which implies a "bilayer" structure in which the side chains would overlap in an antiparallel interdigitated structure. The smectic A–smectic C transition involves expansion in the plane orthogonal to the polymer chains. The interpenetration of the side groups disappears but the side chains tilt down with respect to the normal to the layer planes to stack closer. Below 150–145 °C the sample crystallizes and in the oriented form can be indexed on an orthorhombic unit cell with a = 35.7 Å, b = 17.85 Å, and c (fiber axis) = 9.85 Å. This doubling of the 4.9-Å chain repeat has been reported for other polyphosphazene structures and can arise from alternating perturbations of the side chains or a change in the backbone conformation.

Introduction

There is considerable interest in side-chain liquid crystalline polymers because the structure can be varied in numerous ways to influence the type of mesophase and physical properties. In these polymers, the "monomeric" mesogen appears as a pendant group attached to the main chain by a flexible spacer. This type of connection preserves the delicate interactions between the pendant liquid crystalline moieties, by decoupling the motion of the main chain from that of the pendant group. Detailed reviews[1-4] have appeared, laying stress upon the role of the flexibility of the main chain, the length of the spacer, the chemical character of the mesogen unit itself on the liquid crystalline phase type, phase stability, and other considerations.

Most of the side-chain liquid crystalline polymers that have been prepared to date have contained polysiloxane, polyacrylate, or polymethacrylate main chains. More recent studies on the effect of the backbone flexibility now include the use of flexible poly(ethylene oxide)[5] or more rigid poly(α-chloroacrylate) chains.[6]

Poly(organophosphazenes) comprise an important class of polymers that possess inherent skeletal flexibility.[7-9] Earlier studies have shown that certain poly(organophosphazenes) with trifluoroethoxy and simple aryloxy side chains are capable of forming an intermediate state of order.[10-13] Wunderlich has classified these polyphosphazenes as "condis crystals".[14] Thermotropic mesophases in polysiloxane and polyphosphazenes have recently been reviewed.[15] As part of a continuing effort to probe the limits of molecular structure compatible with liquid crystallinity, preparation of novel polyphosphazenes containing mesogenic side groups separated from the main chain by a flexible group has also been reported.[16-19] In this paper we will describe the synthesis and structure determination, thermal analysis, optical microscopy, and X-ray diffraction data for the polymer of structure I, prepared as shown in Scheme I.

Experimental Section

Materials. Hexachlorocyclotriphosphazene (II) (Ethyl Corp.) was purified by recrystallization from *n*-heptane followed by vacuum sublimation at 90 °C (0.1 Torr). Poly(dichlorophosphazene) (III) was prepared by the ring-opening polymerization of II at 245 °C for 108 h and isolated in 20% yield according to procedures previously described.[20] Tetrahydrofuran (THF) was dried over sodium benzophenone ketyl and distilled over dry nitrogen before use. Toluene was distilled from CaH_2. Reagent grade cyclohexane and pentane were stored over 4-Å molecular sieves prior to use. Sodium hydride, NaH, as a 60% dispersion in oil (Aldrich), was washed several times with cyclohexane, filtered, washed with pentane, and stored over nitrogen prior to use.

Mesogen Synthesis. The diazo coupling reaction between 4-*n*-butylaniline and phenol was used for the preparation of 4-((*n*-butylphenyl)azo)phenol. The compound was recrystallized from cyclohexane to give the product in 75% yield: mp 80.5 °C (lit.[21] mp 81 °C); ^{1}H NMR ($CDCl_3$) δ 7.7–7.9 (m, ArH), 7.2–7.4 (m, ArH), 6.9–7.1 (m, ArH), 2.75 (t, CH_2Ar), 1.2–1.9 (br m, CH_2CH_2), 0.95 (t, CH_3); mass spectrum, m/z 254 ($C_{16}H_{18}N_2O$, 254), 211, 161, 133, 121, 93.

Preparation of 2-(4-((*N*-Butylphenyl)azo)phenoxy)ethanol. A solution of 2-chloroethanol (2.37 mL, 0.036 mol) in eth-

† Current address: U.S. Army Natick RD+E Center, Natick, MA 01760.
‡ Laboratoire de Physicochimie Structurale et Macromoleculaire.
§ Laboratoire de Physique des Liquides et Electrochimie.

0024-9297/91/2224-0510$02.50/0

Scheme I

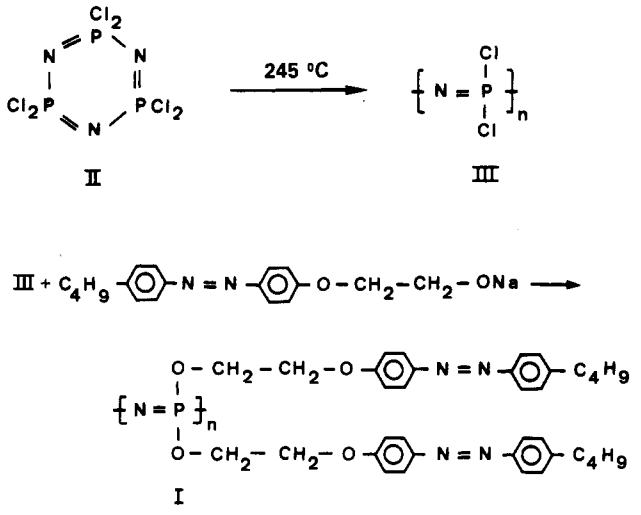

anol (20 mL) was added dropwise to a mildly heated solution of 4-((*n*-butylphenyl)azo)phenol (3.0 g, 0.012 mol), sodium hydroxide (1.42 g, 0.036 mol), and potassium iodide (1.96 g, 0.012 mol) in ethanol (100 mL). Upon completion of the addition, the reaction was refluxed for 16 h. After cooling, the reaction mixture was combined with methylene chloride (125 mL), washed with dilute sodium hydroxide and water, and dried over magnesium sulfate. Upon evaporation of the solvent, fine, orange needlelike crystals of the desired azo alcohol were isolated (3.18 g, 89%). This material was recrystallized from cyclohexane: mp 97 °C (lit.[17] mp 97 °C).

Preparation of $[NP(OCH_2CH_2OC_6H_4N{=}NC_6H_4C_4H_9)_2]_n$ (I). A suspension of sodium 2-(4-((*n*-butylphenyl)azo)phenoxy)-ethoxide in THF (100 mL), prepared from 2-(4-((*n*-butylphenyl)-azo)phenoxy)ethanol (21.07 g, 0.071 mol) and sodium hydride (1.70 g, 0.071 mol), was maintained under a dry nitrogen atmosphere. A toluene solution (70 mL) of poly(dichlorophosphazene) (III) (2.72 g, 0.023 mol) was added dropwise, and the reaction mixture was maintained at reflux for 16 h with vigorous stirring. The product was isolated by precipitation into methanol and washed several times with water to remove NaCl. The weight of recovered product I was 10.31 g (63% yield). This product was twice dissolved in THF and precipitated with methanol prior to vacuum-drying for analysis: IR (cm^{-1}) 3052, 2955, 2927, 2872 (w, ArCH), 1420 (w, N=N), 1253 (s, PN); ^1H NMR ($CDCl_3$) δ 7.7–7.9 (m, ArH), 7.2–7.4 (m, ArH), 6.9–7.1 (m, ArH), 3.9–4.2 (m, OCH_2CH_2O), 2.75 (t, CH_2Ar), 1.2–1.9 (br m, CH_2CH_2), 0.95 (t, CH_3). Molecular weight analysis: light scattering $\bar{M}_w = 1.7 \times 10^6$; intrinsic viscosity, $[\eta]$ = 1.3 dL/g. Anal. Calcd for $C_{36}H_{42}N_5O_4P$: C, 67.59; H, 6.62; N, 10.95; P, 4.84. Found: C, 67.53; H, 6.73; N, 11.08; P, 5.08; Cl, 0.0090.

Analytical Techniques. Proton NMR spectra in $CDCl_3$ with Me_4Si as an internal standard were obtained with a Perkin-Elmer Model R32 90-MHz spectrometer. Mass spectral data were obtained with a Hewlett-Packard 5995C mass spectrometer using a direct insertion technique and electron ionization at 70 eV. Infrared (KBr disk) spectra were recorded on a Perkin-Elmer 1740 FTIR spectrometer.

The thermal transitions were measured by means of a Du Pont 1090 thermal analyzer with a DSC 910 attachment. All samples were under 15 mg and were both heated and cooled at 10 °C/min.

The transition characteristics were surveyed with a polarizing microscope (Olympus BHA-P) equipped with a Mettler FP-5 hot stage.

Densities of the crystalline samples were measured by flotation in mixtures of carbon tetrachloride and acetone.

X-ray diffraction patterns were recorded on flat films using Cu Kα radiation. A flat graphite crystal with a pinhole collimator was used as a monochromator. The samples were contained in 1-mm Lindemann glass tubes which were mounted in an electrically heated oven, the temperature of which was controlled within 0.2 °C, using a platinum resistor as a sensing element.

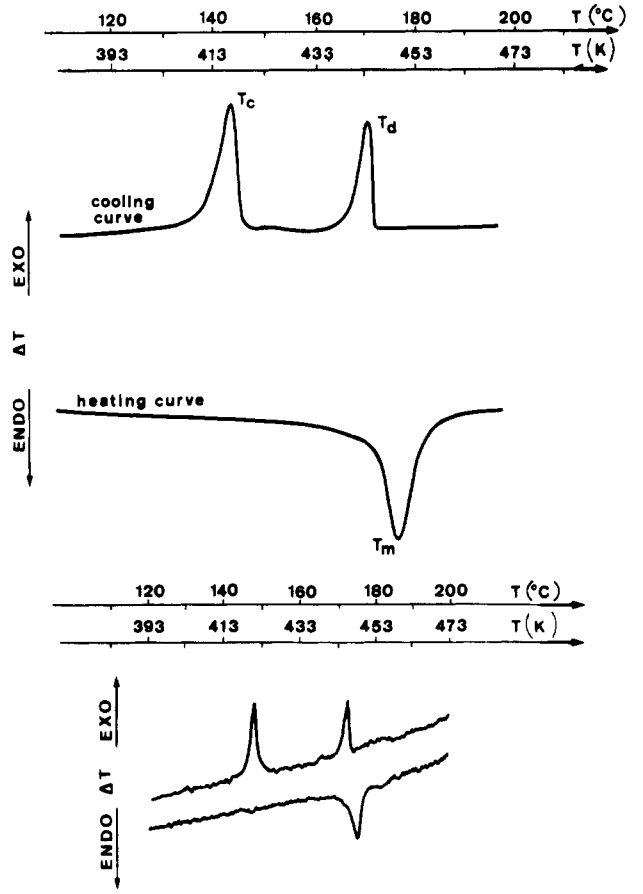

Figure 1. DSC heating and cooling curves for polymer I: (a) 10 °C/min; (b) 2 °C/min. T_m = melting, T_c = crystallization, and T_d = deisotropization temperature.

Well-oriented samples were produced by drawing fibers out of the mesophase with a pair of tweezers.

Results and Discussion

Differential Scanning Calorimetry. Figure 1a shows the DSC curves of polymer I obtained on analysis by DSC for consecutive heating and cooling cycles. In the first heating, apart from the glass transition at ca. 80 °C, only one broad endotherm is seen at T_m = 177 °C (ΔH_m = 2.45 kcal·mol^{-1}, ΔS_m = 5.45 cal·mol^{-1}·K^{-1}).

Upon cooling, two exothermic transitions are observed at T_d = 171 °C (ΔH_d = 1.14 kcal·mol^{-1}, ΔS_d = 2.57 cal·mol^{-1}·K^{-1}) and T_c = 144 °C (ΔH_c = 2.3 kcal·mol^{-1}, ΔS_c = 5.5 cal·mol^{-1}·K^{-1}). In addition, a small exotherm is seen in the temperature range 156–150 °C. The onset of crystallization is sharply defined and occurs at a supercooling of ca. 33 °C, as indicated by the interval between the melting (T_m) and recrystallization (T_c) peaks. It is to be noted that the temperature interval is reduced as the cooling rate is decreased (Figure 1b). At a scanning rate of 2 °C/min the transition temperatures are T_m = 176, T_d = 173, and T_c = 148 °C. These changes are summarized as follows: first heating, $T_g \sim$ 80 °C, T_m = 177 °C, ΔH_m = 2.45 kcal·mol^{-1}, ΔS_m = 5.45 cal·mol^{-1}·K^{-1}; first cooling, T_d = 171 °C, ΔH_d = 1.14 kcal·mol^{-1}, ΔS_d = 2.57 cal·mol^{-1}·K^{-1}, $T_{SA/SC}$ = 156–150 °C, T_c = 144 °C, ΔH_c = 2.3 kcal·mol^{-1}, ΔS_c = 5.5 cal·mol^{-1}·K^{-1}.

On the second heating (Figure 2), the broad endotherm separates into a double peak at 173 and 177 °C and a small isotropization peak at 185 °C. Further cooling and heating cycles only marginally affect the DSC curves.

Optical Microscopy. Upon heating polymer I for the first time, no fluidity can be detected by optical microscopy, and no typical texture can be obtained below 170 °C. At

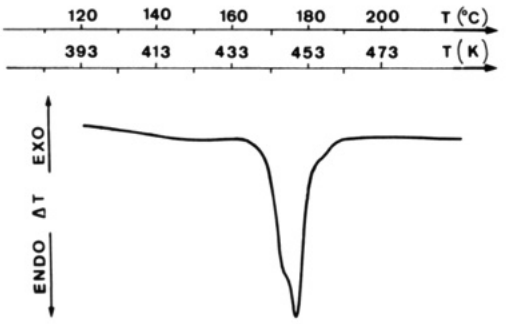

Figure 2. Second heating cycle after cooling to room temperature at 10 °C/min.

a

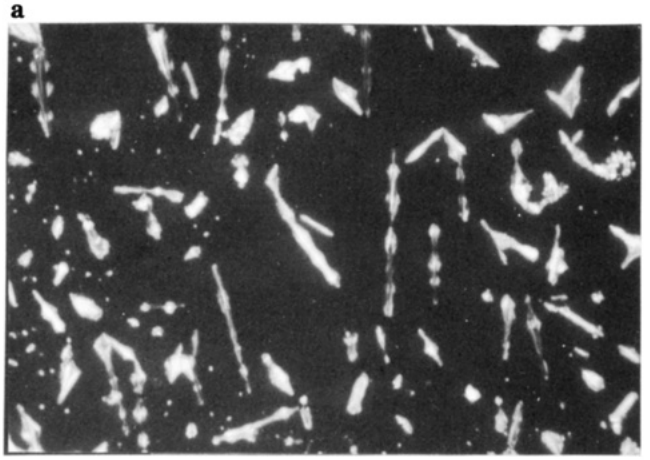

b

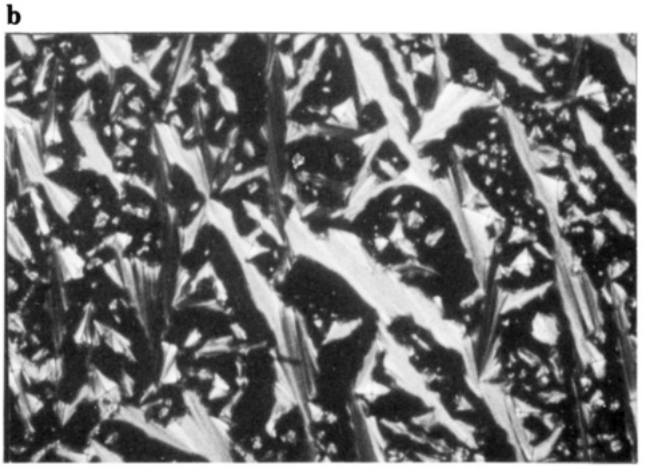

Figure 3. Separation of the smectic phase in the form of batonnets from the isotropic liquid of polymer I: (a) 167 °C; (b) 162.7 °C. Crossed polarizers; original magnification 200× (the photomicrographs have been reduced to 60% of the original size for publication purposes).

this temperature the onset of melting occurs but birefringence persists up to 187 °C, the isotropization temperature.

Upon cooling from the isotropic liquid, a mesophase begins to re-form at the deisotropization point, T_d, in the form of "batonnets" (Figure 3a) which, after further cooling, grow (Figure 3b), coalesce, and reorganize their shape until a final texture is established (Figure 4). This texture is similar to the classical focal conic fan texture exhibited by low molar mass smectics A. Textural changes occur at ca. 156 °C (Figure 5) suggesting the existence of a second smectic mesophase. Then, little or no change is shown by the texture on cooling to room temperature. However, at ca. 150–145 °C, the mechanical displacement of the coverslip becomes difficult, indicating that the polymer is solidifying.

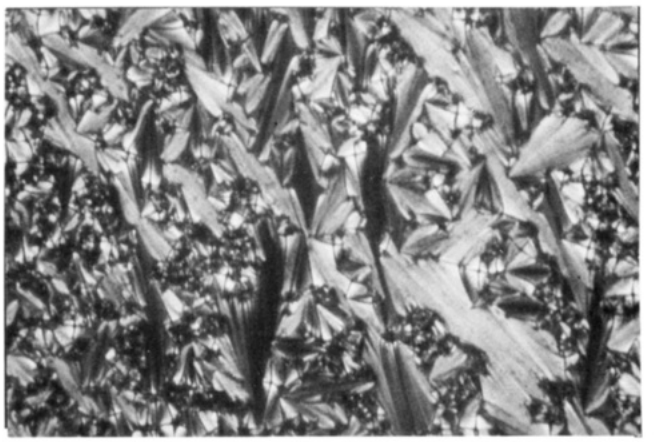

Figure 4. Focal conic fan texture of the smectic phase of polymer I at 158.7 °C. Crossed polarizers; original magnification 200× (the photomicrograph has been reduced to 60% of the original size for publication purposes).

Figure 5. Texture of polymer I at 152 °C. Crossed polarizers; original magnification 200× (the photomicrograph has been reduced to 60% of the original size for publication purposes).

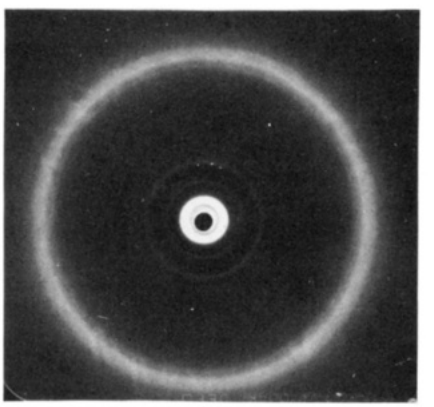

Figure 6. X-ray diffraction pattern of powder sample taken at room temperature.

X-ray Diffraction. Powder Samples. X-ray diffraction patterns of powder samples were obtained up to 200 °C, the temperature at which degradation of polymer I is relatively fast. At room temperature, polymer I is essentially crystalline in character. The X-ray patterns (Figure 6) present several well-defined rings corresponding to the lattice spacings given in Table I. Six of the nine observed reflections can be indexed, within experimental error, as orders of a 35.7-Å spacing. The reflection at 9.93 Å is close to the value reported for the chain-axis repeat (*c* spacing) of related polyphosphazenes[22,23] and our own value from oriented samples (see next section). From these data alone, we are unable to confidently propose all unit cell parameters.

Table I
Lattice Spacings Determined from X-ray Patterns of Powder Samples at Room Temperature Indexed as Orders of 35.7 Å

d, Å	orders of 35.7 Å	d_{calcd}, Å
35.7	1	35.7
17.7	2	17.85
11.87	3	11.90
9.93[a]		
8.95	4	8.92
7.21	5	7.14
6.44		
4.63		
4.41	8	4.46

[a] This value is close to the value of 9.85 Å deduced for the c-axis (chain axis) repeat from oriented samples but can also be indexed by the orthorhombic unit cell discussed in the section on oriented samples.

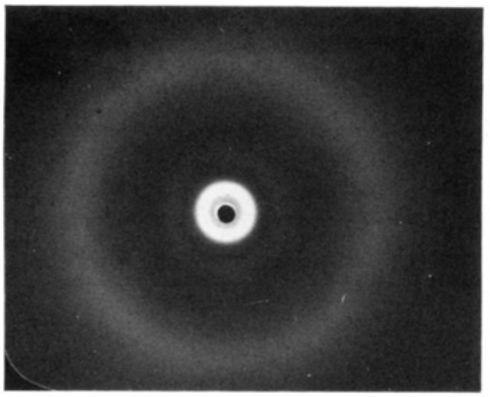

Figure 7. X-ray diffraction pattern of powder sample taken at 180 °C.

Heat treatment above 80 °C noticeably increases the crystallinity of the sample. Then, the X-ray patterns do not change with increasing temperature up to 170 °C, a temperature close to the melting point. A further slight increase in temperature results in a transformation of the X-ray patterns. They present two inner rings (d = 29.5 and 11.6 Å), which are found to be twice as broad as the rings observed in the crystalline state. In addition, there is a relatively sharp outer ring at 4.4 Å. From the first reflection (d = 29.6 Å), one can infer that a contraction of the structure occurs in the plane orthogonal to the polymer chain, assuming an orthorhombic unit cell. Within a narrow temperature range covering ca. 2–5 °C, the outer line is replaced by a diffuse halo centered on a spacing of 4.65 Å, while the first reflection shifts to lower d values (Figure 7). At ca. 180 °C, the X-ray patterns are characterized in the wide-angle region by a diffuse halo and in the small-angle region by two rings corresponding to spacings of ca. 25.5 and 11.6 Å. The diffuse halo is associated with the average lateral approach distance of the side chains (4.65 Å). The diffuse line (d = 11.6 Å) remains unchanged through the whole temperature range and may be due to some intramolecular interference. The small-angle ring (d = 25.5 Å) indicates a lamellar structure; the stacking period is in excess of the length of the side chain calculated from standard bond lengths and angles under the assumption of an all-trans conformation ($L \sim$ 20 Å) but less than twice the extended molecular length. This gives rise to two possible models for the side-chain ordering: (1) a smectic A-like structure in which the side chains would overlap in an antiparallel, interdigitated structure or (2) a tilted smectic C-like ordering.

It should be noted that optical microscopy does not reveal any smectic C characteristics at this temperature. Therefore, the system would have smectic A-like properties.

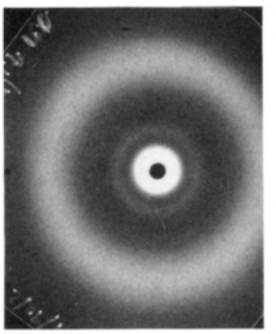

Figure 8. X-ray diffraction pattern obtained from sample preheated at 195 °C in the isotropic liquid phase and then cooled to 160 °C.

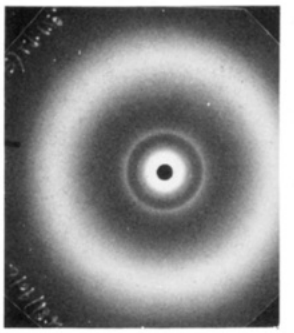

Figure 9. X-ray diffraction pattern obtained from sample preheated at 195 °C in the isotropic liquid phase and then cooled to 152 °C.

Above 200 °C, degradation occurs during the time required to record the scattered intensity as indicated by the appearance of extra rings at 6.05, 5.40, 3.78, and 3.46 Å. It should be noted that depolymerization is known to occur in polyphosphazenes with prolonged heating at high temperatures.[24,25]

The X-ray diffraction patterns obtained from samples preheated at 195 °C in the isotropic liquid phase and then cooled to 160 °C are similar to those previously described. They consist of a broad, diffuse outer ring at ca. 4.65 Å, indicating a lack of periodic lateral order, and two inner rings at d = 25.8 and d = 11.7 Å (Figure 8). Again, these results are consistent with a disordered smectic A-like structure, in agreement with both optical and thermal measurements.

The X-ray diffraction patterns obtained from samples preheated at 195 °C and then cooled to 152 °C are different, which is in agreement with the transition observed by DSC and optical microscopy in the temperature range 156–150 °C. The two inner rings are replaced by sharp rings at 36.39, 17.98, 12.00, and 7.28 Å (close to the orders of the fundamental), which are also found in the crystalline state. The intensity sequence of these reflections is strong, weak, medium, and very weak, respectively. In addition, the outer halo becomes sharper (Figure 9). These results indicate a conversion to a mesophase of higher order. The structural transformation involves expansion in the plane orthogonal to the polymer chains. The interpenetration of the side groups observed at higher temperatures tends to disappear, and the structure possesses ordered packing of parallel polymer chains. However, disorder in the longitudinal direction remains and accounts for the outer halo. With unoriented samples it was impossible to draw an inference on this disordered lamellar structure. We will show later that data on oriented fibers have removed this indetermination and argued for a smectic C-like structure. Such an identification is in agreement with the small exotherm observed upon cooling in the temperature range 156–150 °C. The enthalpies associated with S_A–S_C

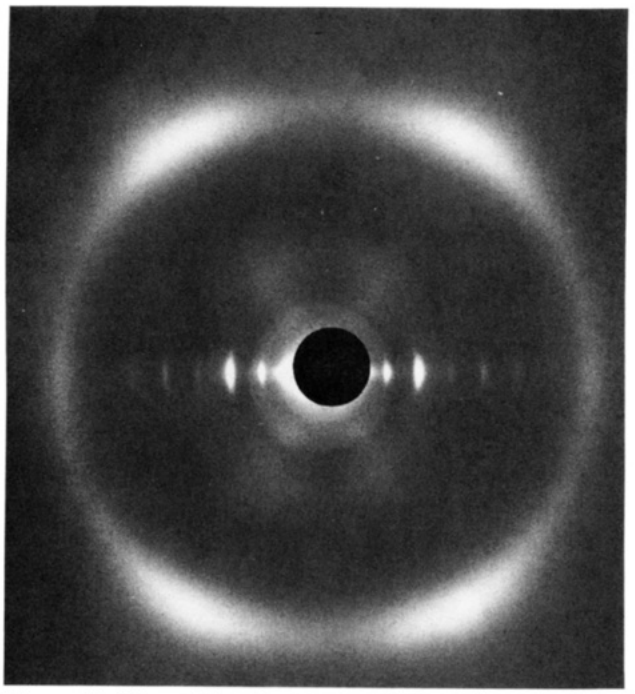

Figure 10. X-ray diffraction pattern of oriented sample drawn from the liquid crystalline state and quenched in water to room temperature. Orientation direction vertical.

transitions are often very small, and the transitions may go undetected. The approximate enthalpy values for low molar mass liquid crystals are of the order 0.1 kcal·mol^{-1} or less.[26]

Samples preheated at 195 °C and then cooled below 140 °C are essentially crystalline in character. The outer halo is replaced by sharp rings, indicating a high order in the longitudinal direction. The X-ray patterns present several well-defined rings corresponding to the lattice spacings given in Table I.

Oriented Samples. The anisotropy shown in the X-ray patterns of oriented samples (Figures 10–12) clearly demonstrates that molecular orientation can be achieved by drawing fibers from the mesophase.

As shown in Figure 10, there are two basic features to note in the X-ray pattern of oriented fiber drawn from the liquid crystalline state and quenched in water to room temperature: (1) a series of equatorial arcs that are all orders of 36.2 Å (the first eight consecutive orders are observed, although the eighth order at spacing 4.53 Å is overlaid by a broader halo at approximately the same spacing); (2) a diffuse four-point, wide-angle pattern with reflections centered on a spacing 4.4 Å and lying on a layer line with spacing 4.9–5.0 Å.

These data are in qualitative agreement with the X-ray diffraction pattern obtained for a powder sample of polymer I preheated at 195 °C and then cooled to 152 °C (Figure 9), indicating that the low-temperature mesophase has been frozen in the glassy state upon rapid quenching in water.

It is worth noting that the X-ray pattern shown in Figure 10 is qualitatively like those for oriented samples of low molar mass smectics C[27] and closely resembles those obtained for side-chain liquid crystalline polymers using oriented fibers drawn from the smectic C phase and rapidly quenched in the glassy state.[28]

The small-angle arcs correspond to the eight first orders of reflection on the layer planes ($d \sim 36.2$ Å). They are located on the equator, which indicates that the smectic layers, and as a consequence the main chains, are parallel to the fiber axis. It is worth comparing the layer spacing,

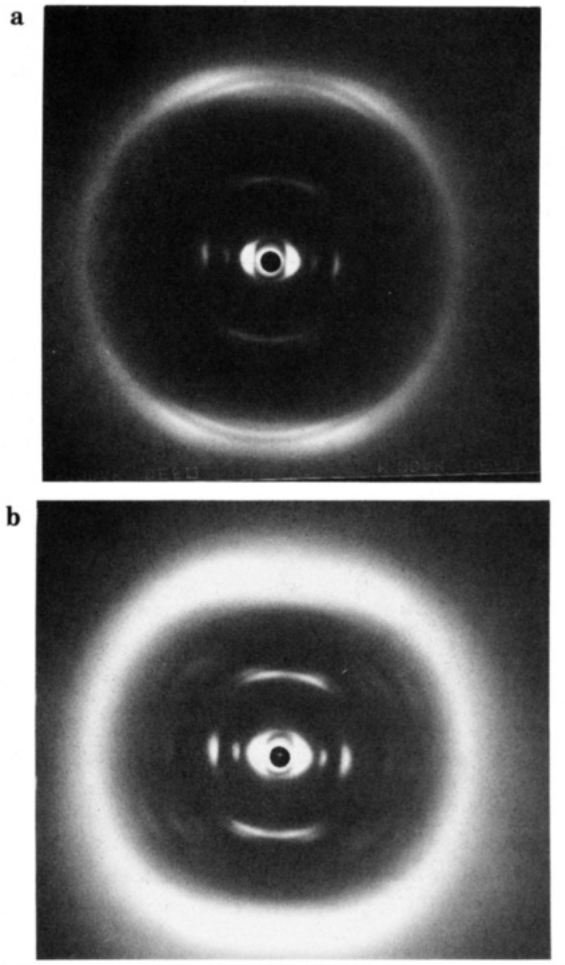

Figure 11. X-ray diffraction pattern of oriented samples drawn from the liquid crystalline state and allowed to cool to room temperature. Exposure times: (a) 16 h; (b) 24 h. Orientation direction vertical.

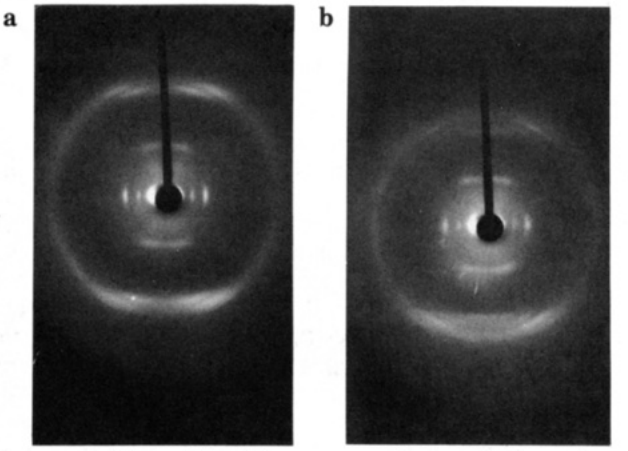

Figure 12. X-ray diffraction patterns of oriented fibers taken at (a) 165 °C and (b) 168 °C. Orientation direction vertical.

d, with the extended model length ($L \sim 20$ Å). It is clear that d is in excess of L so that some form of bilayer structure is implied.

The four diffuse crescents at large angles are associated with the unstructured liquidlike nature of the layers. They are roughly equidistant from the origin and lie on a layer line with spacing 4.9 Å, which is similar to the values reported previously for a series of polyphosphazenes: a chain repeat distance (c) of 4.9 Å was found, which has been attributed to a planar or alternating cis–trans backbone.[15,29-32] Formally, the backbone structure is a 2_1 helix. The diffuse crescents form pairs aligned on straight

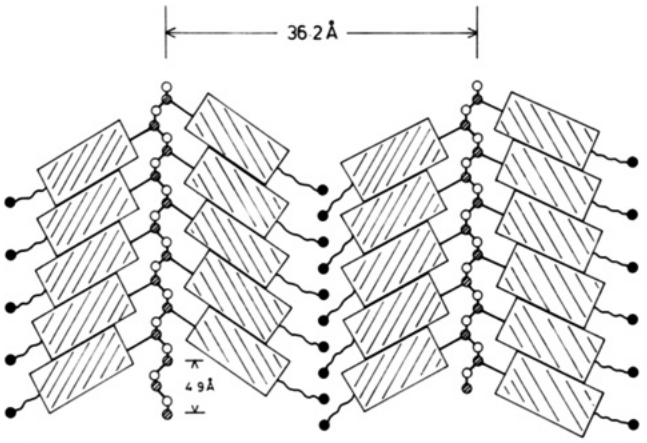

Figure 13. Schematic diagram to illustrate structural criteria needed to explain basic features of oriented X-ray pattern shown in Figure 10. The phosphorus (crosshatched circles)–nitrogen (open circles) backbone is in the planar cis–trans conformation with a repeat of 4.9 Å and is separated from the next chain by 36.2 Å. The aromatic mesogen units in the side chain (crosshatched boxes) tilt down by 26° to give a perpendicular separation of 4.4 Å. The length of the extended side chains is ca. 20 Å. The diagram is a projection: in practice, two side chains emanate from each phosphorus atom. The terminal methyl groups are denoted by solid circles.

lines making an angle of ca. 20–30° with respect to the fiber axis. Therefore, we can conclude that the mesogenic side groups are tilted with respect to the layer planes. The two distinct orientations for the mesogenic side groups can be readily explained as shown schematically in Figure 13. In this model, the two side chains attached to a given phosphorus atom hang on the same side of the polymer backbone. However, regarding the configuration of the pairs of pendant groups with respect to the main chain, these are typically described as emerging alternatively from opposite sides of the polymer backbone in a kind of herringbone arrangement. This allows the side chains to stand at an approach distance of ca. 4.4 Å, compatible with their steric hindrance and their chemical repeat distance along the backbone. Polymer backbones are thought to lie in essentially parallel planes within the smectic layers. Concerning the stacking of the smectic layers, it is worth noting that both the powder (Figure 9) and fiber (Figure 10) X-ray patterns show no evidence of *hkl* reflections. Hence, three-dimensional correlations between the layers are either absent or extremely weak.

All the above-mentioned data are consistent with a smectic C-like structure. It is quite unusual, however, to observe eight orders of reflection in the scattering patterns of a thermotropic smectic C phase.

Recently, for a series of four side-chain polysiloxanes in the smectic A state, Davidson et al.[33] reported oriented diffraction patterns characterized by a large number of Bragg reflections on the smectic layers as compared to other thermotropic polymers such as polyacrylates or polymethacrylates. The most characteristic feature for polysiloxanes is to possess a flexible backbone with a large electron density because of the silicon atoms. From the intensities of the different Bragg reflections, Davidson et al. inferred that the projection of the electron density profile along the normal to the layers cannot be described by the ideal model of a single sinusoidal modulation commonly used for low molar mass liquid crystals.[34] The density profiles were in agreement with smectic layers divided into sublayers consisting of the aliphatic tails, the mesogenic cores, and the flexible spacers, respectively, the polymer backbones being strongly confined in a sublayer of width 6 ± 2 Å along the director. Similar

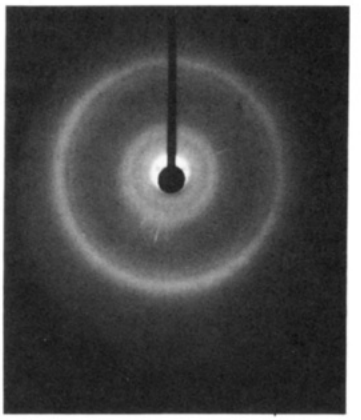

Figure 14. X-ray diffraction patterns taken at 172 °C. Molecular orientation achieved by drawing fibers is not preserved at this temperature.

considerations apply to interpretation of the data for polymer I, which also possesses a flexible backbone with a large electron density because of the phosphorus atoms. The eight orders of reflection on the smectic layers reflect the influence of the polyphosphazene chains on the electron density profile: the polymer backbone appears strongly squeezed between the other sublayers. From the model proposed for the tilted packing in Figure 13, a crude estimate of the electron density profile along the normal to the layers can be obtained by dividing for each chemical structural subunit (backbone, spacer, mesogenic core, and terminal substituent) the total number of electrons by the projected length. The results thus obtained are in qualitative agreement with the intensity sequence of the small-angle reflections.

If oriented fibers are allowed to cool slower to room temperature, then crystallization occurs as shown in Figure 11. Heat treatment at and above 130 °C significantly increases the crystallinity. The effect of annealing is shown in Figure 12. Along the meridian line (fiber axis) two symmetrical sharp arcs can be observed. They correspond to a spacing of 9.85 Å, twice that of 4.9 Å. The doubling of the polymer chain repeat with respect to the usual $(cis,trans)_2$ 4.9 Å is consistent with four monomer units linked in a nearly planar fashion. As discussed by Brukhart et al.[22] and Meille et al.[23] for poly[bis(3,4-dimethylphenoxy)phosphazene] (PDMP) and poly[bis(4-isopropylphenoxy)phosphazene] (PDPP), respectively, the 9.85-Å distance is compatible with two models for the backbone, namely, a $(trans,trans,trans,cis)_2$ $(T_3C)_2$ or a $(trans,cis)_4$ $(TC)_4$ geometry. A structure refinement is necessary before attempting to delineate between the two conformations. Buckhart et al.[22] preferred the $(T_3C)_2$ structure for PDMP, and Meille et al.[23] favored the $(TC)_4$ structure for PDPP accounting for a doubling of the c repeat by alternating the spatial arrangement of the side groups. The X-ray patterns present along the equator several sharp spots, namely, a fundamental and higher order reflections corresponding to a distance of ca. 35.7 Å, slightly contracted from the 36.2 Å in Figure 10. Additional diffraction signals are seen off the equator and the meridian which allow us to determine the third unit cell parameter. All the present data are consistent with an orthorhombic cell; trial parameters were refined by an alternative least-squares procedure, and final values are a = 35.7, b = 17.85, and c = 9.85 Å.

Unfortunately, the molecular orientation of the stretched fibers was not preserved throughout the heating cycle because of the fluid properties of the polymer I at 171 °C (Figure 14).

The calculated density for a two-chain unit cell is 1.35 g/mL, which compares favorably with the measured

density of 1.25 g/mL. It is worth comparing this measured density with the value reported by (i) Bishop and Hall[31] for crystalline oriented poly[bis(*p*-chlorophenoxy)phosphazene] (PDCP) of 1.54 g/mL and (ii) Matsuzawa et al.[32] for poly[bis(*p*-fluorophenoxy)phosphazene] (PBFP) of 1.42–1.45 g/mL, depending on the annealing temperature. In our case, with a greater proportion of $(CH)_2$ groups and also a lower proportion of heavier atoms (F, Cl) in the side chain, we would expect a lower density for the crystalline phase, and the value of 1.25 g/mL is comparable with that reported by Meille et al.[23] for PDPD of 1.20 g/mL. In all cases reported, the calculated density is greater than the measured density, which is the normal expectation.

Conclusion

Polarized optical studies, and the DSC and X-ray diffraction results show that polymer I exhibits the following polymorphism:

	Crystal–smectic C-like structure	smectic A-like structure	isotropic liquid
upon heating:	~170/173 °C	~177 °C	~185/187 °C
upon cooling:	~144/148 °C	~156 °C	~171 °C

Oriented fibers obtained by slow cooling from the liquid crystalline state possess an orthorhombic structure (a = 35.7 Å, b = 17.85 Å, c = 9.85 Å). The fiber repeat period of 9.85 Å is consistent with four monomer units linked in a nearly planar fashion.

X-ray diffraction patterns obtained with powder samples in the low-temperature mesophase are characteristic of a disordered lamellar structure. The average lateral spacing between the side chains is ca. 4.4 Å. This corresponds approximately to the average width of the side chains but is smaller than the diameter of a freely rotating molecule, which is consistent with most results reported so far for a variety of thermotropic side-chain liquid crystalline polymers. The layer thickness is 36.2 Å, indicating the formation of a bilayer structure. More detailed structural information was extracted from the X-ray pattern of an oriented fiber drawn in the mesophase and quenched in water to freeze the structure in the glassy state. A separation of the structure into sublayers must be considered: strong lateral interactions of the paired mesogenic units lead to a close packing of the mesogens in layers and rejection of the polyphosphazene backbone from this array. The polymer backbones are thought to be highly confined and to lie in essentially parallel planes within perpendicular smectic C layers of the side chains. Pairs of side chains occur every 2.45 Å along the polymer backbone but the congestion is relieved in the cis–trans conformation when the stacking periodicity becomes 4.9 Å. Pairs of mesogens emerge alternatively from opposite sides of the polymer backbone in a "herringbone" arrangement. The disorder in the main chain and the flexibility of the spacer allow the mesogenic side groups to order in a parallel manner and to tilt with respect to the normal to the layer planes to stack closer. Evidence for the herringbone structure comes from the four-point wide-angle pattern shown in Figure 10, which shows four arcs and a set of equatorial 36.2-Å signals.

The structure of the high-temperature mesophase is closely related to the smectic C-like structure described above. Again, the mesogenic side groups are parallel to one another and are arranged in layers. However, the mesogenic groups are perpendicular to the planes of the layers and overlap in an antiparallel, interdigitated smectic A-like structure.

It is worth noting that the schematic arrangements proposed for the polyphosphazene backbone and the aromatic azo mesogenic side groups in the smectic phases of polymer I are similar to the models reported recently for polysiloxanes containing two mesogenic units attached through one flexible spacer to each silicon atom.[35,36]

Acknowledgment. We acknowledge suggestions during the course of this study from Professor Robert Lenz, University of Massachusetts, and Ms. Marie Potts, Army Materials Technology Laboratory, for viscosity and light scattering measurements. R.S. thanks Dr. Nathaniel Schneider and Dr. Richard Desper, Army Materials Technology Laboratory, for their review and comments on the manuscript.

References and Notes

(1) Finkelmann, H.; Rehage, G. *Adv. Polym. Sci.* **1984**, *60/61*, 99.
(2) Shibaev, V.; Plate, N. A. *Adv. Polym. Sci.* **1984**, *60/61*, 173.
(3) Cser, F.; Horvath, J.; Nyitrai, K.; Hardy, G. *Isr. J. Chem.* **1985**, *25*, 252.
(4) McArdle, C. B., Ed. *Side-Chain Liquid Crystal Polymers*; Blackie, Chapman and Hall: New York, 1989.
(5) Pugh, C.; Percec, V. *Polym. Bull.* **1986**, *16*, 521.
(6) Esselin, S.; Bosio, L.; Noel, C.; Decobert, G.; Dubois, J. C. *Liq. Cryst.* **1987**, *2*, 505.
(7) Allcock, H. R.; Allen, R. W.; Meister, J. J. *Macromolecules* **1976**, *9*, 950.
(8) Allcock, H. R.; Arcus, R. A. *Macromolecules* **1979**, *12*, 1130.
(9) Allcock, H. R.; Arcus, R. A. *Macromolecules* **1980**, *13*, 919.
(10) Allen, G.; Lewis, C. J.; Todd, S. M. *Polymer* **1970**, *11*, 44.
(11) Schneider, N. J.; Desper, C. R.; Singler, R. E. *J. Appl. Polym. Sci.* **1976**, *20*, 3087.
(12) Schneider, N. J.; Desper, C. R.; Beres, J. J. In *Liquid Crystalline Order in Polymers*; Blumstein, A., Ed.; Academic: New York, 1978; p 299.
(13) Kojima, M.; Magill, J. H. *Makromol. Chem.* **1985**, *186*, 649.
(14) Wunderlich, B.; Grebowicz, J. *Adv. Polym. Sci.* **1984**, *60/61*, 1.
(15) Godovsky, Y. K.; Papkov, V. S. *Adv. Polym. Sci.* **1989**, *88*, 131.
(16) Kim, C.; Allcock, H. R. *Macromolecules* **1987**, *20*, 1726.
(17) Singler, R. E.; Willingham, R. A.; Lenz, R. W.; Furukawa, A.; Finkelmann, H. *Macromolecules* **1987**, *20*, 1727.
(18) Allcock, H. R.; Kim, C. *Macromolecules* **1989**, *22*, 2596.
(19) Percec, V.; Tomazos, D.; Willingham, R. A. *Polym. Bull. (Berlin)* **1989**, *22*, 199.
(20) Singler, R. E.; Hagnauer, G. L.; Schneider, N. S.; LaLiberte, B. R.; Sacher, R. E.; Matton, R. W. *J. Polym. Sci., Polym. Chem. Ed.* **1974**, *12*, 433.
(21) Steinstraesser, R.; Pohl, L. *Z. Naturforsch. B* **1971**, *26* (6), 577.
(22) Burkhart, C. W.; Gillette, P. C.; Lando, J. B.; Beres, J. J. *J. Polym. Sci., Polym. Phys. Ed.* **1983**, *21*, 2349.
(23) Meille, S. V.; Porzio, W.; Allegra, G.; Audisio, G.; Gleria, M. *Makromol. Chem., Rapid Commun.* **1986**, *7*, 217.
(24) Allcock, H. R.; More, G. Y.; Cook, W. J. *Macromolecules* **1974**, *7*, 571.
(25) Hagnauer, G. L.; LaLiberte, B. *J. Appl. Polym. Sci.* **1976**, *20*, 3073.
(26) Gray, G. W.; Goodby, J. W. *Smectic Liquid Crystals*; Leonard Hill: Glasgow, 1984.
(27) Leadbetter, A. J.; Norris, E. K. *Mol. Phys.* **1979**, *38*, 669.
(28) Decobert, G.; Dubois, J. C.; Esselin, S.; Noel, C. *Liq. Cryst.* **1986**, *1*, 307. Freidzon, Ya. S.; Talroze, R. V.; Boiko, N. I.; Kostromin, S. G.; Shibaev, V. P.; Plate, N. A. *Liq. Cryst.* **1988**, *3*, 127.
(29) Giglio, E.; Pompa, F.; Ripamoti, A. *J. Polym. Sci.* **1962**, *59*, 293.
(30) Allcock, H. R.; Kugel, R. L.; Stroh, E. G. *Inorg. Chem.* **1972**, *11*, 1120.
(31) Bishop, S. M.; Hall, I. H. *Br. Polym. J.* **1974**, *6*, 193.
(32) Matsuzawa, S.; Yamaura, K.; Tanigami, T.; Higuchi, M. *Colloid Polym. Sci.* **1985**, *263*, 888.
(33) Davidson, P.; Levelut, A. M.; Achard, M. F.; Hardouin, F. *Liq. Cryst.* **1989**, *4*, 561.
(34) De Gennes, P. G. *The Physics of Liquid Crystals*; Clarendon Press: New York, 1974.
(35) Diele, S.; Hisgen, B.; Reck, B.; Ringsdorf, H. *Makromol. Chem., Rapid Commun.* **1986**, *7*, 267.
(36) Diele, S.; Oelsner, S.; Kuschel, F.; Hisgen, B.; Ringsdorf, H.; Zentel, R. *Makromol. Chem.* **1987**, *188*, 1993.

Registry No. 4-*n*-Butylaniline, 104-13-2; phenol, 108-95-2; 4-((*n*-butylphenyl)azo)phenol, 2496-21-1; 2-(4-((*n*-butylphenyl)-azo)phenoxy)ethanol, 130934-28-0; 2-chloroethanol, 107-07-3.